Measurement of the top quark Yukawa coupling from tt kinematic distributions in the dilepton final state with the ATLAS experiment

C. Garvey[1], **J. Keaveney**[1]

[1]Physics, University of Cape Town, Cape Town, South Africa

E-mail: GRVCAM001@myuct.ac.za

Abstract. An extraction of the top quark Yukawa coupling (Y_t) from top quark pair production is presented using proton-proton collisions at 13 TeV, corresponding to an integrated luminosity of 140 fb^{-1}, recorded by the ATLAS experiment. Corrections from a Higgs boson exchange between the top quark and top anti-quark can produce non-negligible modifications to differential distributions near the energy threshold of production. The kinematic distributions sensitive to these modifications, are the invariant mass of the system ($m_{t\bar{t}}$) and the azimuthal angle of the top quark with respect to the beamline in the rest frame of the system. This analysis aims to constrain Y_t indirectly using the kinematic distributions of $t\bar{t}$ pair events using the eμ dilepton final state. Machine learning was used to reconstruct the mass of the top quark system as this provides the greatest sensitivity to variations in Y_t. A binned profile likelihood fit was then implemented to extract a blinded estimation of Y_t using Asimov data including a complete set of statistical and systematic uncertainties. The extracted Y_t^2 = 1.00$\pm$1.73 and is systematically limited

1 Introduction

Since the discovery of the Higgs boson by ATLAS[1] and CMS[2], a key focus of the LHC physics program has been to precisely determine the properties of the Higgs boson, including its mass and coupling strengths with Standard Model (SM) particles. Of these couplings, the top quark yukawa coupling±(Y_t) is of particular interest. As the most massive SM particle, the top quark is expected to have the largest Yukawa coupling, close to unity. This large coupling means that top quark loops contribute significantly to radiative corrections of the Higgs potential, which affect theoretical predictions such as the stability of the electroweak vacuum[3]. There are two approaches used to measure the Y_t, which are direct and indirect. The direct method aims to measure processes where top quarks are produced in association with a Higgs boson, such as . The indirect approach measures processes where a virtual Higgs is exchanged between top quarks, such as in $t\bar{t}$. The work presented focuses on the indirect measurement of Y_t from the kinematic distributions of $t\bar{t}$ in the dilepton channel. Figure 1 presents the Feynman diagrams of $t\bar{t}$ production with leading order (LO) electroweak (EW) corrections where a virtual Higgs is exchanged between the top quark and top antiquark. The virtual exchange of a Higgs enhances $t\bar{t}$ production near the threshold energy hence affecting the kinematics of the $t\bar{t}$ system. These affects allow one to infer the strength of Y_t. This inference utilises the impact that varying Y_t has on the kinematic distributions of the $t\bar{t}$ system. It will thus prove important to access observables that are sensitive to these variations. The analysis focuses on dilepton $t\bar{t}$ which follows the decay chain $t\bar{t} \rightarrow bW^+\bar{b}W^- \rightarrow b\ell^+\nu_\ell\bar{b}\ell^-\nu_\ell$. Specifically we are targetting the case where there is exactly one electron and one muon. It is required to also have two jets that originate from bottom quarks.

The paper will be presented as follows. Firstly, I will introduce the data and simulation that are used, followed by the selection criteria put in place to preferentially select for eμ $t\bar{t}$ production. I will then outline the EW corrections that were implemented to the $t\bar{t}$ simulation to allow for the variation of Y_t. A discussion of the methods used to construct observables that are sensitive to variations in Y_t is then provided. Finally, the results of the extraction are presented.

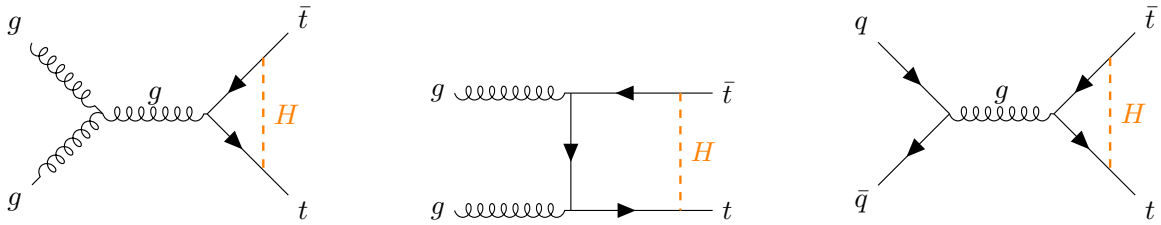

Figure 1: Feynman diagrams showing the LO electroweak corrections to $t\bar{t}$ production involving the virtual exchange of a Higgs boson. The left and middle diagrams show $t\bar{t}$ as initiated by gluon-gluon while the right shows qq initiated.

2 Simulation and event selection

The data used was recorded from proton-proton collisions at the LHC with $\sqrt{s}$ = 13 TeV, using the ATLAS experiment. The dataset corresponds to Run 2 and covers the data-taking period from 2015 to 2018. The total integrated luminosity corresponds to 140 fb^{-1} [4].

To accurately model the data recorded in the dilepton channel, we need to include simulation of all physics processes that can pass our selection criteria. The signal simulation is a dilepton $t\bar{t}$ simulation produced using ATLAS full simulation with POWHEG[5]. and PYTHIAV8.230[6], at NLO in QCD. Apart from the signal process, $t\bar{t}$, several background processes are expected to pass the selection criteria. The dominant background contribution is due to tW with a subdominant contribution from Z+jets. The tW process is simulated usingPOWHEG v.2 and PYTHIA v8.309 at NLO in QCD. The process including a Z boson in association with additional jets is simulated using SHERPA 2.2.11[7]. It is important to note that $t\bar{t}$, tW and Z+jets cover the dominant and sub-dominant processes that pass our selection criteria but this does not cover all processes that could pass our selections. It is, however, expected that the remaining processes are expected to have a negligible impact on the analysis.

The selections put in place for the dilepton eμ channel are as follows. For an event to be included in this analysis it needs to have passed either a single electron or single muon trigger. It is then required that there are exactly two leptons, one electron and one muon, each with a transverse momentum (p_T) of greater than 28 GeV. It is also required that there are at least two jets with a p_T greater than 20 GeV. Of the required jets within the event it is required that at least two of the jets are tagged as having originated from a bottom quark using the `DL1d` b-tagger[8]. Finally, it is required that the dilepton mass ($m_{\ell\ell}$ is greater than 10 GeV to minimise the contributions from low mass resonances.

3 Electroweak corrections

The simulation of $t\bar{t}$ is implemented at next-to-leading order in QCD and as such, does not include the necessary EW corrections such as those shown in Figure 1. The calculations of the EW corrections to $t\bar{t}$ production is described in [9] and have been implemented using `HATHOR`[10]. The corrections are implemented by first calculating the differential $t\bar{t}$ cross section including the LO QCD contributions as well as the mixed contributions of order $\alpha_S^2\alpha_{weak}$. The calculations are computed in terms of variables sensitive to variations in Y_t and correspond to the invariant mass of the $t\bar{t}$ system ($m_{t\bar{t}}$) and the azimuthal angle of the top quark with respect to the beam line in the rest frame of the $t\bar{t}$ system known as $\cos\theta^*$. The ratio of the calculated cross section including the EW contributions to the LO QCD cross section is then computed and binned in terms of a double differential distribution of $m_{t\bar{t}}$ and $\cos\theta^*$. To apply the correction a multiplicative weight $\omega(m_{t\bar{t}},\cos\theta^*)$ is defined from the differential distribution and requires access to the kinematics of the top quarks. At this point it is important to define truth and detector level within simulation. Truth level refers to the stage immediately after the matrix element calculation, involving quarks and gluons before hadronisation, whereas detector level includes the simulation of final-state particles after hadronisation, decay, and their interaction with the ATLAS detector. To apply the weight $\omega(m_{t\bar{t}},\cos\theta^*)$ it is necessary to accesses the truth information for each event to compute the $m_{t\bar{t}}$ and $\cos\theta^*$. This is done for each of the gg, $u\bar{u}$, $d\bar{d}$ initial. Figure 2 shows the effects of varying Y_t on the distributions where the values of Y_t =0, 1, 2, 3 are used. The x-axis shows the truth level $m_{t\bar{t}}$ and the y-axis of the upper panel shows the expected number of events. The y-axis on the lower panel shows the ratio of each of the Y_t varied histograms to the histogram with Y_t =1. Larger deviations from a ratio of one indicate a greater sensitivity to variations in Y_t. From figure 2 it can be seen that the majority of the sensitivity to variations in Y_t arises when the energy of the $t\bar{t}$ system is approximately

twice m_{top} and is known as the threshold region.

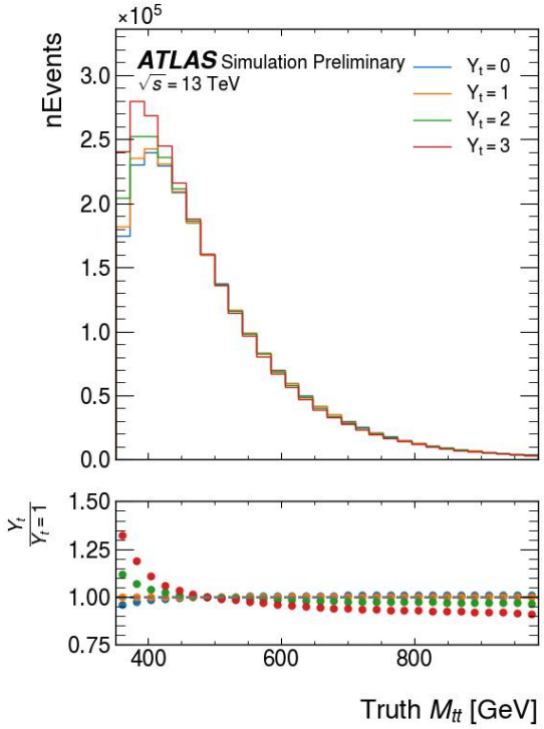

Figure 2: A histogram showing the variations of Y_t as a function of truth level m_{tt} for the $t\bar{t}$ simulation in the eμ channel. The lower panel shows the ratio of each of the Y_t varied histograms to the histogram with Y_t =1.

4 Construction of kinematic observables sensitive to variations in Y_t

The variables that were found to be most sensitive to variations in Y_t at truth level were the m_{tt} and $\cos\theta^*$. These variables are not directly accesible at detector level due to the inability to detect neutrinos. As such, several observables were tested, which aimed to work as proxy variables for the m_{tt}. The first and simplest attempt involved using the measurable decay products of the top quarks, namely the two leptons and two b-jets, and calculating the combined invariant mass ($m_{\ell\ell bb}$). Using the $m_{\ell\ell bb}$ observable provided a severely degraded sensitivity when compared to the truth level m_{tt}. To this end, a deep neural network (DNN) was used to regress and reconstruct the truth m_{tt} using information available at detector level. The DNN was implemented using `Keras` and was trained on $t\bar{t}$ simulation. A set of eighteen physics inspired variables were defined for training the DNN. These variables were the mass and δR of the different lepton-b-jet combinations as well as the missing transverse momentum. Figure 3a shows a normalised histogram of the difference between the reconstructed m_{tt} and the truth level m_{tt} in the eμ channel. The y-axis shows the fraction of events and the mean and σ of the distribution are 14.75 and 111.01. From figure 3a it can be inferred that the reconstructed m_{tt} is on average slightly larger than the truth level m_{tt}. Overall the bias of the reconstruction is minimal.

Figure 3b shows the Y_t variations as a function of the m_{tt} reconstructed using the DNN. The description of the y-axes and the lower panel is the same as found in figure 2. From the lower panel in figure 3b the sensitivity to variations in Y_t can be seen. The reconstructed m_{tt} was found to be more sensitive than the $m_{\ell\ell bb}$ but less sensitive than the truth m_{tt}.

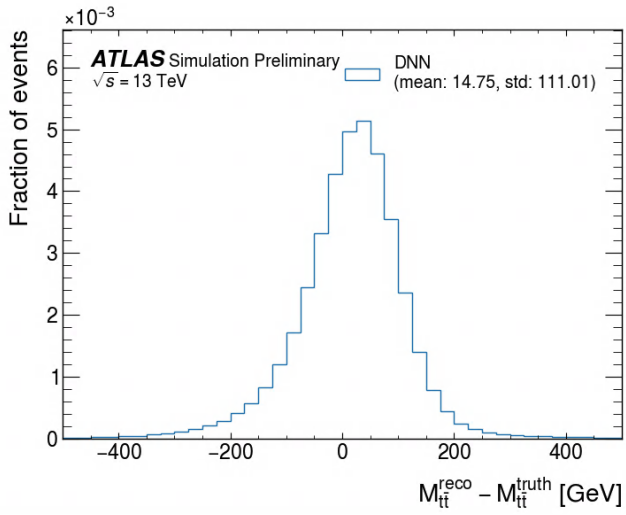

(a) Figure 3a shows a normalised histogram of the difference between the reconstructed m_{tt} and the truth level m_{tt}.

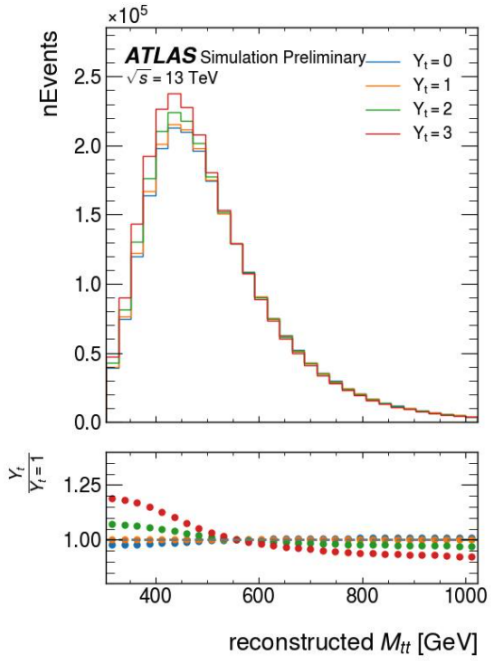

(b) A set of histograms showing the variations of Y_t for the reconstructed m_{tt}. The lower panel in each figure shows the ratio of each of the Y_t varied histograms to the histogram with Y_t =1.

Figure 3: Figures showing the output of the training of the DNN when comparing the truth m_{tt} and reconstructed m_{tt} and the sensitivity of the reconstructed m_{tt} when Y_t is varied.Both plots are shown for in the eμ channel.

5 Fit methodology and results

A binned profile likelihood fit was used to extract the Y_t. To extract the best fit value for Y_t, the fit must include a parametric dependency where varying the value of Y_t directly controls the shape of the chosen kinematic distribution. This is implemented using a method known as template morphing. The template morphing method uses a set of histograms where each histogram corresponds to a specific values of Y_t and linearly interpolates between the bins of each the histograms to allow Y_t to continuously vary within the fit. The templates used in the fit correspond to the histograms given in figure 3b each for the different values of Y_t =0,1,2,3. It should be noted that due to technical considerations the Y_t^2 is extracted instead of Y_t. A complete set of systematic uncertainties are considered including detector and theoretical systematics. The results shown are fully blinded and the fit is performed using Asimov data [11]. Table 1 shows the extracted values for Y_t^2 when using the $m_{\ell\ell bb}$ and the reconstructed $m_{\mathrm{t\bar{t}}}$ distributions. The uncertainties quoted include both statistical and systematic uncertainties

Variable	**Extracted Y_t^2**
$m_{\ell\ell bb}$	1.00 ± 1.73
Reconstructed $m_{\mathrm{t\bar{t}}}$	1.00 ± 1.56

Table 1: A table summarising the extracted values for Y_t^2 when using different variables. The uncertainties quoted include both statistical and systematic uncertainties

The extracted values of Y_t^2 =1 is expected as we are using Asimov data. Comparing the fits results of the fits using the $m_{\ell\ell bb}$ and the reconstructed $m_{\mathrm{t\bar{t}}}$ distribution it can clearly be seen that there is a reduction in the uncertainty when using the reconstrcuted $m_{\mathrm{t\bar{t}}}$. This reduction provides a strong indication that reconstructing the truth $m_{\mathrm{t\bar{t}}}$ using a DNN provides an increase in sensitivity to the variations in Y_t. This analysis is systematically limited where the dominant systematic uncertainties are due to the $\mathrm{t\bar{t}}$ modelling and the b-tagging.

6 Conclusion

An extraction of the top quark Yukawa coupling from top quark pair production is presented using proton-proton collisions at $\sqrt{s}$ = 13 TeV, corresponding to an integrated luminosity of 140 fb^{-1}, recorded by the ATLAS experiment. The analysis focused on the dilepton channel and specifically the case where there is one electron and one muon. An event selection was applied to enhance the contribution of dileptonic $\mathrm{t\bar{t}}$ events while minimising background contributions. The $\mathrm{t\bar{t}}$ simulation is implemented at NLO in QCD and as such does not contain the necessary EW corrections. These EW corrections were implemented using `Hathor` allowing for the variation of Y_t in $\mathrm{t\bar{t}}$ simulation through the use of a multiplicative event weight. Varying the value of Y_t affects the shape of the kinematic distributions of $\mathrm{t\bar{t}}$ production and decay. To effectively measure Y_t one needs to construct observables that are maximally sensitive to variations in Y_t. Such an observable was constructed using a DNN which allowed for the reconstruction of $m_{\mathrm{t\bar{t}}}$. A blinded fit was then implemented using template morphing and the extracted result was $Y_t^2 = 1.00^{+1.56}_{-1.50}$. The analysis is systematically limited by the $\mathrm{t\bar{t}}$ modelling and b-tagging systematics. The results shown provide an independent determination of the top quark Yukawa coupling. Moving forward the result could be improved by also reconstructing $\cos\theta^*$ and extracting Y_t from a two dimensional distribution of the two variables.

References

[1] ATLAS, "Observation of a new particle in the search for the standard model higgs boson with the atlas detector at the lhc," *Physics Letters B*, vol. 716, no. 1, p. 1–29, Sep. 2012. [Online]. Available: http://dx.doi.org/10.1016/j.physletb.2012.08.020

[2] CMS, "Observation of a new boson at a mass of 125 gev with the cms experiment at the lhc," *Physics Letters B*, vol. 716, no. 1, p. 30–61, Sep. 2012. [Online]. Available: http://dx.doi.org/10.1016/j.physletb.2012.08.021

[3] D. Buttazzo, G. Degrassi, P. P. Giardino, G. F. Giudice, F. Sala, A. Salvio, and A. Strumia, "Investigating the near-criticality of the higgs boson," *Journal of High Energy Physics*, vol. 2013, no. 12, dec 2013. [Online]. Available: https://doi.org/10.1007%2Fjhep12%282013%29089

[4] G. e. a. Aad, "Luminosity determination in pp collisions at $\sqrt{s} = 13$ tev using the atlas detector at the lhc," *The European Physical Journal C*, vol. 83, no. 10, Oct. 2023. [Online]. Available: http://dx.doi.org/10.1140/epjc/s10052-023-11747-w

[5] C. Oleari, "The powheg box," *Nuclear Physics B - Proceedings Supplements*, vol. 205-206, pp. 36–41, 2010, loops and Legs in Quantum Field Theory. [Online]. Available: https://www.sciencedirect.com/science/article/pii/S0920563210001994

[6] T. e. a. Sjöstrand, "An introduction to pythia 8.2," *Computer Physics Communications*, vol. 191. [Online]. Available: http://dx.doi.org/10.1016/j.cpc.2015.01.024

[7] E. e. a. Bothmann, "Event generation with sherpa 2.2," *SciPost Physics*, vol. 7, no. 3, Sep. 2019. [Online]. Available: http://dx.doi.org/10.21468/SciPostPhys.7.3.034

[8] "Neural Network Jet Flavour Tagging with the Upgraded ATLAS Inner Tracker Detector at the High-Luminosity LHC," CERN, Geneva, Tech. Rep., 2022. [Online]. Available: https://cds.cern.ch/record/2839913

[9] J. H. Kühn, A. Scharf, and P. Uwer, "Weak Interactions in Top-Quark Pair Production at Hadron Colliders: An Update," *Phys. Rev. D*, vol. 91, no. 1, p. 014020, 2015.

[10] M. Aliev, H. Lacker, U. Langenfeld, S. Moch, P. Uwer, and M. Wiedermann. Hathor version 2.1-b3. [Online]. Available: https://www.physik.hu-berlin.de/de/pep/tools/hathor.html

[11] G. Cowan, K. Cranmer, E. Gross, and O. Vitells, "Asymptotic formulae for likelihood-based tests of new physics," *The European Physical Journal C*, vol. 71, no. 2, Feb. 2011. [Online]. Available: http://dx.doi.org/10.1140/epjc/s10052-011-1554-0